A study of the canopy effect on fire regime transition using an objectively defined Byram convective number

Kai Zhang, Salman Verma, Arnaud Trouvé, Aymeric Lamorlette

Version of Record: https://www.sciencedirect.com/science/article/pii/S0379711219304497
Manuscript_eef95c02c034fb88d7a370f21ec9461c

A study of the canopy effect on fire regime transition using an objectively defined Byram convective number

Kai Zhang[a*], Salman Verma[b], Arnaud Trouve[b], Aymeric Lamorlette[a]

***Corresponding author.**
E-mail address: kai.zhang.1@city.ac.uk

[a]Aix-Marseille University, CNRS, Centrale Marseille, M2P2, 13451, Marseille, France
[b]Department of Fire Protection Engineering, University of Maryland, College Park, MD, 20742, USA

Abstract
Forest fires can be classified into two regimes, depending on Byram convective number N_C: a plume-dominated and wind-driven regime. This classification is often based on two-dimensional (2D) studies without considering flame front structures, and is associated with the change of governing heat transfer mechanism. Studies based on three-dimensional (3D) considerations suggest the dependency of the fire regime transition on canopy characteristics $CdLAI$ ($C_d\alpha_s\sigma_s H_F/2$) through which the atmosphere boundary layer (ABL) flow changes to mixing layer (ML) flow. Hence, the primary objective of the present study is to investigate the fire regime transition and its associated heat transfer mechanisms with the aid of drawing a dimensionless configuration space {N_C, $CdLAI$}. This requires an objective definition of the Byram convective number; the $2m$ or $10m$ high open wind speed ($U_\infty = U_2$ or U_{10}) often used to define it being arbitrary. Therefore, the present study introduces a scaling method for the reference height (Y_{ref}) at which the wind speed U_{ref} is chosen to define a new Byram convective number N_C'. A mathematical expression for Y_{ref} as a function of canopy/vegetation height is proposed for a small-scale, stationary fire. The new configuration space {N_C', $CdLAI$} is considered more suitable for investigating the fire regime transition.

Keywords
ForestFireFOAM; CFD; combustion; multiphase; pine needle; heat transfer

Nomenclature

C_d	Drag coefficient
C_P	Specific heat capacity of ambient air
g	Gravitational acceleration
H_F	Vegetation height
I, I_{rad}	Fireline intensity, radiation intensity
J	Irradiance
LAI	Leaf area index
N_C, N_C'	Byram and new Byram convective number
R	Total buoyancy power
T_∞, T_s, T	Temperature of ambient air, solid and gas
U_∞, U_{ref}	Open wind speed, reference wind speed
Y_0, Y_{ref}	Ash thickness and reference height where U_{ref} is defined

Greek symbols

α_g, α_s	Volume fraction of gas and solid
σ_s	Surface to volume ratio (SVR)
ρ_∞	Density of ambient air

1. Introduction

Investigating the governing heat transfer mechanisms from radiative (plume-dominated) to convective (wind-driven) is of primary interests in fire science community because of the dependency of flame properties such as rate of spread (ROS) on heat transfer mechanisms.

Nelson [1] tabulated five convective numbers representing the criteria [2, 3] often used to classify three heat transfer mechanisms: the radiative, convective and mixed heat transfer. The Byram convective number N_C, which properly classified the governing heat transfer mechanisms of previous experimental fires [4], can be written as,

$$N_C = \frac{2gI}{\rho_\infty (U_\infty - ROS)^3 C_P T_\infty} \tag{1}$$

Where ρ_∞, C_P and T_∞ are the density, specific heat and temperature of the ambient air. I is the fireline intensity and U_∞ is often defined as $2m$ or $10m$ high open wind speed (U_2 or U_{10}) [5, 6]. It was concluded that for N_C<2, a wind-driven fire, which has a large tilt angle, is dominated by convective heat transfer. For N_C >10, radiation takes over the role of preheating the vegetation that a plume-dominated fire has tilt angle smaller than 20º. Mixed radiative and convective heat transfer mechanism occurred at 2< N_C <10. This general observation was confirmed by Morvan and Frangieh [7] in whose paper the data of laboratory fires at various conditions are re-visited.

Despite the wide use of N_C in fire science community, unique dependency of the fire regime transition and governing heat transfer mechanism on this parameter is questioned. From a physical point of view, forest fire propagation through vegetation experiences two flow behaviors, an ABL and a ML flow occur behind and in front of the flame front respectively. The ABL flow, which develops on the burnt vegetation layer (rough ashes), can be described by the log-law wind profile [8] (see (2)), while the ML flow develops on unburnt vegetation. In fact, N_C can be used to represent ABL flow behavior; and $CdLAI$, an exclusive property of canopy recognized in fire science community [9, 10], represents the behavior of ML flow. Theoretically, ahead of the fire propagating front where canopy is unburnt, ABL to ML transition occurs roughly at $CdLAI = 0.1$, *i.e.*, for $CdLAI$<0.1, canopy layer has ignorable impact on ABL flow; whereas for $CdLAI$>0.1, representing dense canopy, an apparent inflection velocity is often observed near the top of canopy layer. A number of simulation works have tried to understand the fire regime transition and heat transfer mechanisms at different wind speeds and vegetation characteristics [11-15]. While, these studies have not systematically considered the dependency of the fire regimes on the ABL to ML flow transition governed by the configuration space {N_C, $CdLAI$}, and are often based on 2D considerations.

In the present study, a 3D large eddy simulation (LES) of a small-scale, carbon-monoxide-fueled stationary fire, which stabilises on a $5m$ long vegetation layer, is performed using a wall-adapting local eddy-viscosity (WALE) turbulence model [16] and eddy dissipation concept (EDC) combustion model [17]. The primary objective of the study is to better characterise the propagating fire regime transition and its associated heat transfer mechanisms with the aid of a dimensionless configuration space {N_C, $CdLAI$}. As an intermediate step, the present paper considers a non-propagating, stationary flame which represents an instantaneous state of a spreading fire as suggested in the work of Verma and Trouve [18]. This allows a prerequisite problem to be solved, that is, the unnecessary implicit dependency of fireline intensity on wind speed. A scaling method, which can be used to find a more objective reference height at which wind speed is chosen to re-define N_C, will be introduced in the next section with a detailed problem description.

2. Problem Description and Methodology

The underlying assumption behind the primary objective of this study is that the N_C and *CdLAI*, which compose the configuration space, have independent impacts on the fire regime transition. That means two conditions must be satisfied: first, for a typical *CdLAI*, N_C can independently decide the fire regime transition; and second, for a typical N_C, the fire regime transition has a unique dependency on *CdLAI*. The two parameters should not be coupled internally in any manners.

However, this is not the case due to the lack of an objective definition for N_C. Note that from (1), $N_C \sim f(U_\infty)$. The open wind speed, often defined at $2m$ or $10m$ reference height (U_2 or U_{10}) [5, 6], has an extra dependency on surface roughness Y_0 given as,

$$U_\infty(Y) = A \times U_{ref} \times ln(\frac{Y+Y_0}{Y_0}) \tag{2}$$

As a first approximation, Y_0 is evaluated as being equal to one-tenth of the vegetation height H_F due to the rough ashes left from burning solid fuel layer. Hence, $U_\infty(Y = Y_{ref}) = U_{ref} = A \times U_{ref} \times \ln(Y_{ref}/Y_0 + 1)$. The constant A can then be calculated from $A = 1/ln(Y_{ref}/Y_0 + 1)$. Because $N_C \sim f(U_\infty)$, $U_\infty \sim f(Y_0)$, $Y_0 \sim f(H_F)$ and $H_F \sim f(CdLAI)$, the two parameters N_C and *CdLAI* are implicitly coupled. For demonstration purpose, four sample cases relying on a typical configuration space $\{N_C = 5.6,\ CdLAI = 0.01\}$ is provided in Table 1.

The cases, though sharing the same configuration space, implicitly contained different surface roughness due to the reasonable assumption that the roughness of the burnt vegetation (ashes) is one-tenth of the unburnt vegetation height H_F. This leads to completely different wind profiles as shown in Fig. 1. Note that the base case wind speed U_∞ for the plot is evaluated at a reference height of $Y = Y_{ref} = 10H_F$ giving $U_{0.5} = 0.6m/s$, while the labelled N_C is calculated based on $10m$ high criterion.

Table 1. Demonstration cases to show the coupling between N_C and *CdLAI*.

Cases / *Parameters*	$\{N_C = 5.6,\ CdLAI = 0.01\}$			
	Base	Case 1	Case 2	Case 3
$H_F\ (m)$	0.05	0.0334	0.025	0.0167
$\alpha_s\sigma_s(/m)$	4	6	8	12
Y_0/H_F	0.1	0.1	0.1	0.1
$Y_0\ (m)$	0.005	0.00334	0.0025	0.00167

Without any experiments or simulations, one can readily conclude that the configuration space $\{N_C, CdLAI\}$ will not provide a unique fire regime transition or local fire behaviour since the imposed wind profiles are different. In other words, there lacks an objective definition for N_C with which the configuration space can be used to study the fire regime transition. This issue is particularly important for experimentalist to compare their fire behaviour data collected from different sources.

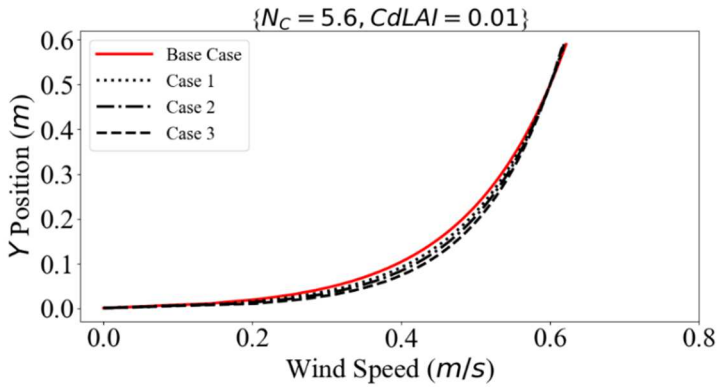

Fig. 1. Boundary layer wind profiles for a typical configuration space.

Therefore, the present study aims at solving the problem by employing a scaling method to re-define the reference height Y_{ref} at which the wind speed U_{ref} can be used to provide an objective definition for N_C (labelled as N_C').

The scaling method is designed following the rule that the new configuration space {N_C', *CdLAI*} should always provide a unique fire behaviour irrespective of vegetation heights and its associated surface/ash roughness, *i.e.*, N_C' and *CdLAI* must be self-independent. The fire behaviour may be described by local flame structure in any reasonable ways that in this study, local buoyancy power $B_y = (\overline{-V''}\,\partial\bar{P}/\,\partial y) + (\overline{-V}\,\partial\bar{P}/\,\partial y)$ in the main flame region (T>500K) is chosen similarly to the work of Verma and Trouve [18]. In that expression, the $q'' = (q - \tilde{q})$, and $\tilde{q}$ ($\bar{q}$) represents density-weighted (ensemble-averaged) quantity. The use of B_y is reasonable because first, local buoyancy power represents the local flame structure changes to the effect of ABL wind; and second, the radiation from the flame body to vegetation layer can be characterized by local flame structures having a temperature higher than 500K. Total buoyancy power in the flame body can then be calculated by spatially integrating B_y along x, y, z-directions (refer to Fig. 3), written as,

$$R = \int_0^{Lx} \int_0^{Ly} (\int_0^{Lz} B_y \, dz) \, dydx \tag{3}$$

Where the lengths Lx and Ly are limited by the temperature condition T>500K, and Lz is the width of the computation domain equals to 0.5m. The use of total buoyancy power R allows a better view of flame structure along the flame extended direction.

To be more specific, the cases in Table 2 are numerically simulated at a reference wind speed $U_\infty(Y = Y_{ref})$ equals to 0.6 *m/s* to obtain the local flame structures depicted by R profiles. The base case retains the assumption that the ABL flow develops on ash thickness Y_0 one-tenth of the vegetation height H_F and the reference height Y_{ref} equals 10H_F.

Table 2. Simplified simulating conditions for scaling reference height Y_{ref} in mixed heat transfer mechanism region (N_C =5.6).

Cases / *Parameters*	$CdLAI = 0.01, H_F = 0.05m,$ $\alpha_s\sigma_s = 4/m, Cd = 0.1$			
	Base	Case 1	Case 2	Case 3
$Y_0\ (m)$	0.005	0.00334	0.0025	0.00167
Y_0/H_F	1/10	1/15	1/20	1/30
Y_{ref}/H_F	10	-	-	-

For small-scale fires such as the one investigated in the present study, these assumptions are reasonable. It is worth highlighting that the use of only one reference wind speed equals to 0.6*m/s* for this study are due to two reasons. First, the fire regime transition from plume-dominated (0.5*m/s*) to wind-driven (0.7*m/s*) occurs roughly at this wind speed (see Fig. 2); and second, the scaling factor introduced for Y_{ref} changes slightly with the reference wind speed. This means the Reynolds number (*Re*) also has slight impacts on fire behaviours, and should be added to the definition of the configuration space. Assuming the fires are strongly turbulent, the *Re* effect (and consequently different reference wind speed) is out of the scope of the present study. Following the often used U_{10} criterion [6], the chosen base case wind speed of 0.6*m/s* corresponds to N_C of 5.6 representing a mixed heat transfer mechanism [1].

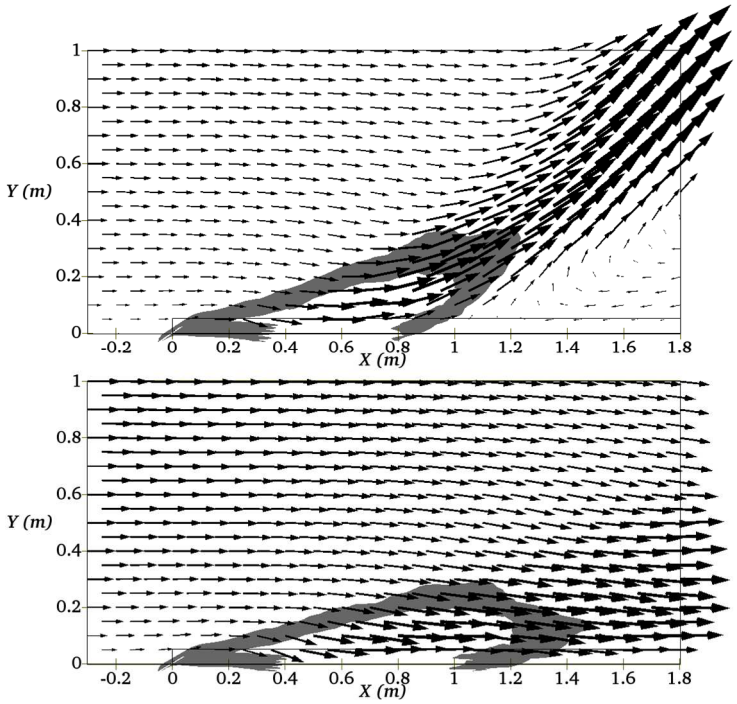

Fig. 2. Mean velocity vectors and 3D flame shapes (T=500K contour) for the reference wind speed $U_{0.5}$ equals to 0.5*m/s* (Top) and 0.7*m/s* (Bottom).

In fact, the cases considered in Table 2 are a simplification of the cases in Table 1. At low $CdLAI = C_d\alpha_s\sigma_s H_F/2$=0.01, the effects of ABL to ML transition on fire behaviours can be ignored because the vegetation is too sparse. The transition will only occur near *CdLAI*=0.1 where an apparent inflection velocity profile was observed at the top of vegetation [19]. It is hence not necessary to have different sets of $\{H_F, \alpha_s\sigma_s\}$ for scaling purposes, *i.e.*, the multiplication of varying H_F and $\alpha_s\sigma_s$ in Table 1 to obtain fixed $CdLAI = C_d\alpha_s\sigma_s H_F/2$=0.01 is not necessary. For instance, assuming an artificial vegetation height $H_F = 10m$ (though not possible), the $\alpha_s\sigma_s$ must be $0.02\,m^{-1}$ in order to retain the *CdLAI*=0.01. Because $\sigma_s = 7500m^{-1}$ is the surface to volume ratio for pine needles, the solid volume fraction $\alpha_s = 0.26 \times 10^{-5}$ is small enough to be ignored. In Table 2, using fixed H_F=0.05m and $\alpha_s\sigma_s$=4/m are sufficient for this study with great simplifications because the volume fraction $\alpha_s = 0.53 \times 10^{-3}$ is also low enough to be ignored. A typical fire behaviour should be theoretically independent of the two low volume fractions as long as *CdLAI* is 0.01 and N_C is fixed.

These lead to the change of Y_0/H_F from 0.1 in Table 1 to different values of Y_0/H_F in Table 2 whilst keep the surface roughness Y_0 unchanged. The two tables are hence essentially equivalent. The cases 1-3 are then used to find new Y_{ref} (or Y_{ref}/H_F) at which the newly defined N_C' has a unique influence on fire regime transition independent of *CdLAI*.

3. Numerical Configurations

A 3D small-scale stationary fire is numerically simulated using an inert vegetation version of compressible solver ForestFireFoam (FFF), an extension of FireFoam solver developed at M2P2 lab, Aix-Marseille University. The FFF solver, which is primarily based on standard Gaussian finite-volume integration method, takes into account the interaction between atmosphere and vegetation invoking a multiphase model [20, 21]. Radiative heat transfer equation is solved using a discrete ordinate method (fvDOM) [22] holding an optically-thin medium assumption. Because the multiphase solver is well elaborated in the literature and validated against experimental fire, a summary of the relevant mathematical equations and models is provided in the Appendix of the present study.

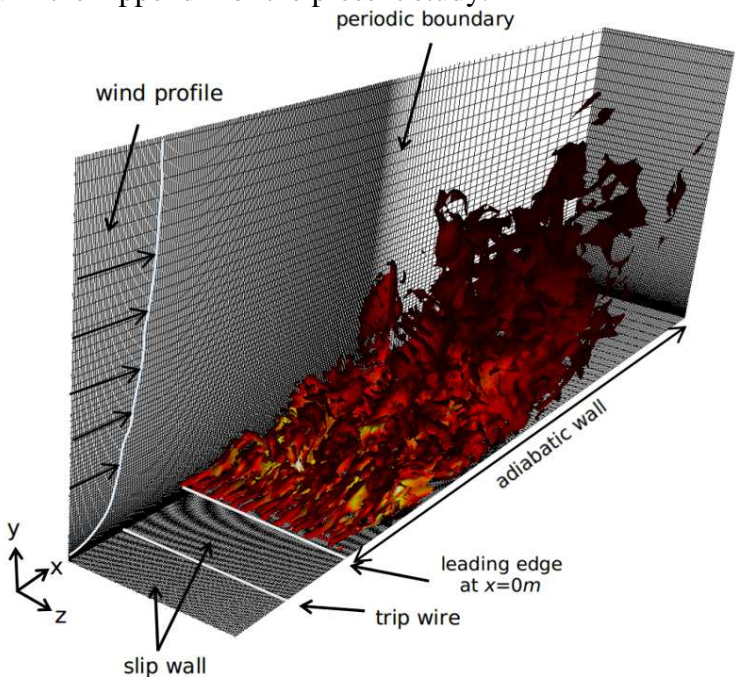

Fig. 3. Visualization of the configuration using instantaneous iso-contour of Q-criterion at $2(s^{-2})$, clipped to $x_{max} = 2.5m$, $y_{max} = 1m$.

The 3D numerical configuration, which is similar to the one used by Verma and Trouve [18], is shown in Fig. 3. The computational domain is $7.8m$ long in streamwise x-direction, $2.5m$ high in the vertical y-direction and $0.5m$ wide in the spanwise z-direction. A burner with its leading edge sitting at $x = 0.0m$ is responsible for the injection of carbon monoxide (CO). This mimics the main product of pyrolysis gas. In the original version of FFF, both pyrolysis and char oxidation can be numerically simulated, while using CO to replace pyrolysis gas in this study greatly reduces computational power required. A trip wire of $0.005m$ long, $0.5m$ wide and $0.005m$ high is placed at $x= (-0.105)m$ to perturb the incoming boundary layer flow given in (2). A slip wall condition is assumed from the left boundary of the computational domain until the leading edge of the burner. From the leading edge of the burner, a vegetation layer of $5m$ long in the x-direction, $0.05m$ high in the y-direction and $0.5m$ wide in the z-direction is imposed. A periodic boundary condition is applied on the walls in the spanwise direction.

A boundary layer wind profile with reference height Y_{ref} equals to $10H_F$ as a base case is imposed on the left entrainment of the domain. The CO injection velocity along vertical y-direction is $0.173636m/s$ corresponding to the fire line intensity I of $100KW/m$.

For the present study, the grid spacing along x-direction roughly equals to $0.005m$ in the main flame region, one third smaller than the cell size (Δ) requirement following the criterion [9],

$$\Delta < \min\left(\frac{H_F}{3}, \frac{2H_F}{LAI}\right) = \min(0.0167m, 0.05m) \quad (4)$$

Where the vegetation height used for the simulation is 0.05m, and the leaf area index LAI ($\alpha_s\sigma_s/2$) is 2 following Table 2. In the y-direction, the size of the first cell close to the bottom wall of the domain is 0.0012m with an expansion ratio of 1.06 up to the height of 0.5m. Considering the overall expansion ratio of the mesh in less important flame region, the total number of cells is 3.5 million. Statistical data is collected using the last 15s out of 30s of the total simulation time. The Courant number is restricted to be smaller than 0.5 using automatic time step adjustment. Each simulation requires CPU time of about 1800h using 32 processors on high performance computing (HPC) cluster of Aix-Marseille University.

4. Results and Discussions

Mean velocity vectors at the plane z=0.0m (a central cutting plane) and 3D flame shapes (T=500K contour) for the base case and case 3 are shown in Figs. 4a and 4b. Although the two cases share the same configuration space $\{N_C = 5.6,\ CdLAI = 0.01\}$ and refer to the same reference height Y_{ref} equals to 10H_F, different flame shapes and local flow structures (particularly near x=1.8m) are clearly observed that the flame extends from 1.35m (base case) to 1.4m (case 3). These different observations for the same configuration space are due to the reason that the wind profiles, which have been shown in Fig. 1, are influenced by not only N_C, but also $CdLAI$. The coupling between the two parameters must be unraveled before the configuration space can be used to study the fire regime transition. As discussed before, the coupling issue can be resolved by looking for a new reference height Y_{ref} at which the wind speed is used to calculate a new N_C. For demonstration purpose, the Y_{ref} equals to 16.25H_F for case 3 is provided in Fig. 4c to compare with the base case in Fig. 4a having the Y_{ref} equals to 10.0H_F. More consistent flame shapes can be observed that the flame length returns from 1.4m to 1.35m, and velocity vectors near x=1.8m are almost identical.

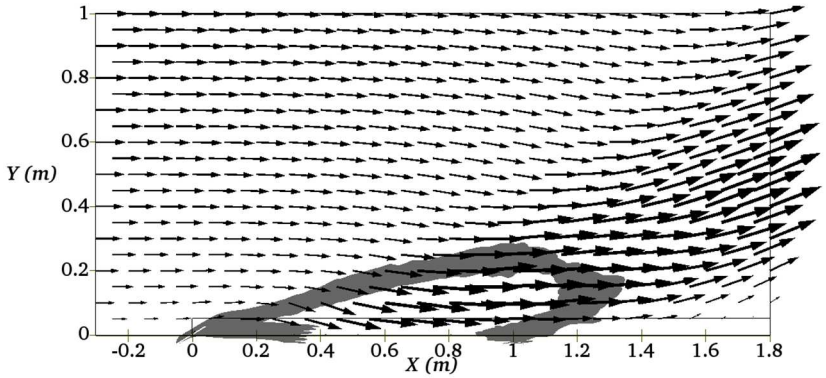

(a) Base case (Y_{ref}/H_F=10.0)

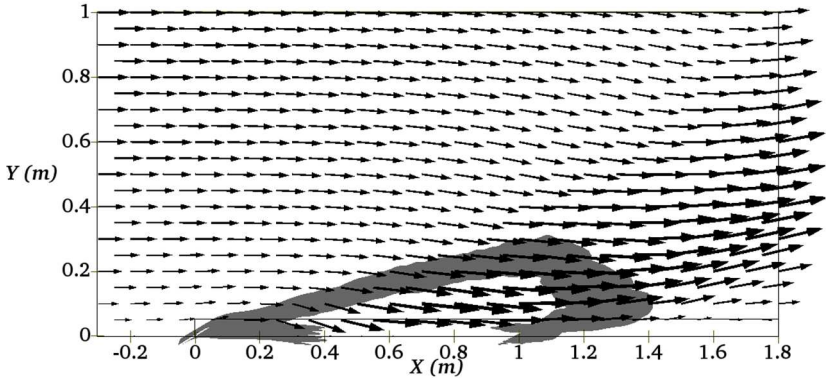

(b) Case 3 (Y_{ref}/H_F=10.0)

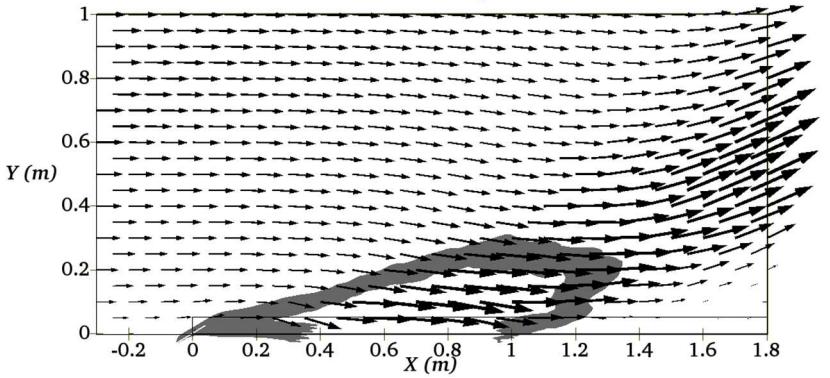

(c) Case 3 (Y_{ref}/H_F=16.25)

Fig. 4. Mean velocity vectors at the plane z=0.0m and 3D flame shapes (T=500K contour) for the configuration space $\{N_C = 5.6,\ CdLAI = 0.01\}$.

In fact, there are difficulties to use velocity vectors or simple 3D flame shapes to compare local fire behaviors for a typical configuration space. Therefore, the R profiles, which are obtained by accumulating the local buoyancy power along x, y, z-directions on the above shown 3D flame shapes, are presented in Fig. 5. The R profiles clearly show that a typical configuration space {N_C=5.6, $CdLAI$=0.01} does not guarantee the same local fire behaviors, and thus can hardly be used to study the fire regime transition. The tip position of the R profile represents the flame length that for case 3, the flame length is about 1.4m consistent with that observed from Fig. 4b. Again, these observations are due to the coupling between N_C and $CdLAI$ via the aforementioned dependencies: $N_C \sim f(U_\infty)$, $U_\infty \sim f(Y_0)$, $Y_0 \sim f(H_F)$ and $H_F \sim f(CdLAI)$.

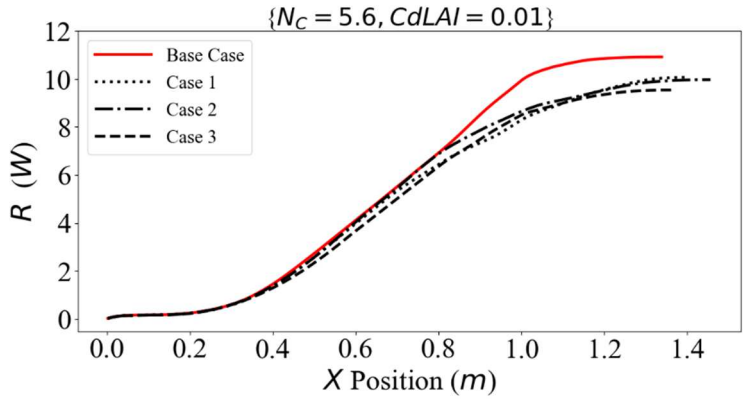

Fig. 5. R profiles base on Y_{ref} equals to 10H_F (without scaling method).

Figure 6 shows the tested new Y_{ref} for cases 1-3 in order to establish a mathematical expression following which an objective N_C', which has no dependency on *CdLAI*, can be defined. Note that not all tested Y_{ref} are shown in the figures, while only those which are useful for the final determination of Y_{ref} are presented. Comparing with the *R* profile for the base case, the best fit *R* profiles for the cases 1-3 are estimated to occur at the ratios Y_{ref}/H_F equal to 12.25, 13.75 and 16.25. For instance, the *R* profiles of case 3, which approximate that of the base case, are bounded by the ratios Y_{ref}/H_F equal to 16.0 and 16.5. This gives an estimation of the best fit *R* profile to occur at Y_{ref}/H_F equals to 16.25. Indeed, as discussed before, the similar flame shapes and flow structures observed in Fig. 4a and Fig. 4c have shown the effectiveness of using the new Y_{ref} to force identical fire behaviours for a typical configuration space.

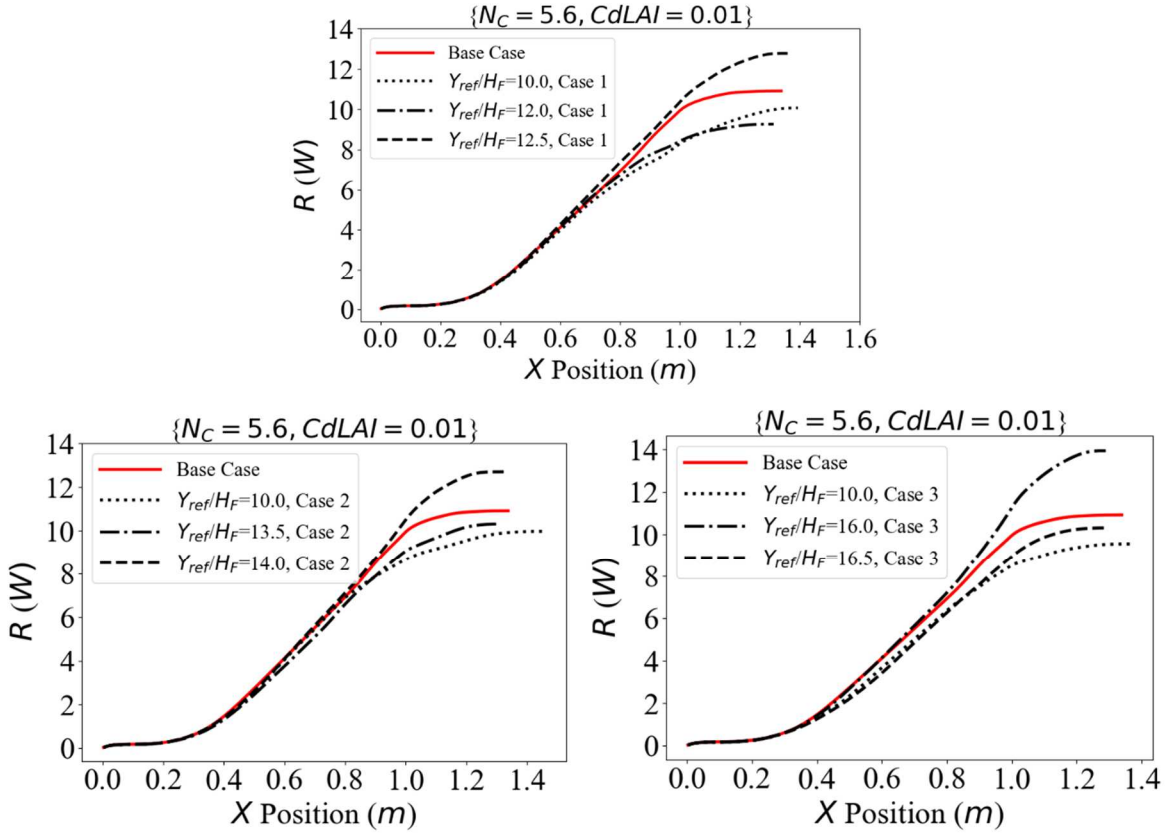

Fig. 6. *R* profiles based on different sets of new Y_{ref} (with scaling method).

Figure 7 presents the best fit curve found for Y_{ref}/H_F as a function of Y_0/H_F, the mathematical expression is given as,

$$\frac{Y_{ref}}{H_F} = -5.66 \ln\left(\frac{Y_0}{H_F}\right) - 3.0774 \tag{5}$$

Following the Table 2 assumption that H_F is $0.05m$ and then the Table 1 assumption that Y_0 is one-tenth of the H_F, the expression can be re-written as,

$$Y_{ref} = -0.283ln(H_F^1) - 0.35 \tag{6}$$

Where the H_F^1 represents the vegetation height from Table 1. The benefit of this expression is that it decouples the N_C from *CdLAI* by forcing the calculation of N_C to rely on different reference heights $Y_{ref} \sim f(H_F^1)$. Therefore, the scaled N_C, written as N_C' can be used to compose a new configuration space {N_C', *CdLAI*}. For a typical *CdLAI* formed by any combinations of $\{H_F, \alpha_s \sigma_s\}$, the new configuration space guarantees a unique fire behaviour or fire regime transition as it entails an objectively defined Byram convective number.

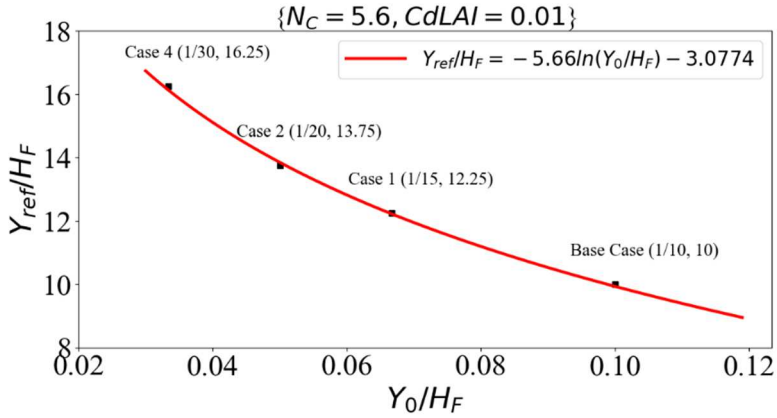

Fig. 7. Mathematical expression and best-fit curve for scaling Y_{ref}.

In fact, writing reference height as a function of vegetation height might be confusing since the chosen canopy/vegetation layer is too sparse to influence the fire behaviour. What has really been removed in the present study is the dependency of wind speed (or consequently N_C) on surface/ash roughness Y_0. The expression in (6) can also be written as,

$$Y_{ref} = -0.283ln(Y_0) - 1.0 \tag{7}$$

The two expressions (6) and (7) are essentially equivalent because Y_0 is directly linked to the vegetation height by $Y_0 = 0.1H_F^1$. These expressions, however, may not be valid for medium or large-scale fires because the base case Y_{ref} equals to $10H_F$ is an assumption that might break down.

Studies are now being performed to search for a mathematical expression for dense vegetation having *CdLAI*=0.5 at which the ML effect on fire regime transition is of our primary interest.

5. Conclusions

A small-scale, carbon-monoxide fuelled stationary fire is simulated using large eddy simulation to introduce the idea of drawing a configuration space {N_C, *CdLAI*} to investigate canopy effect on the fire regime transition. Due to the subjective definition for N_C, a preliminary scaling method is proposed in order to decompose N_C from *CdLAI*. Results show that due to the fact that $N_C \sim f(U_\infty)$, $U_\infty \sim f(Y_0)$, $Y_0 \sim f(H_F)$ and $H_F \sim f(CdLAI)$, local fire behaviours differ in terms of the flame structure represented by *R* profiles and mean velocity vectors for a typical configuration space {N_C=5.6, *CdLAI*=0.01}.

A mathematical expression is therefore introduced that by scaling the reference height at which the wind speed is chosen to calculate Byram convective number, a more objectively defined N_C' can be used to form a new configuration space {N_C', *CdLAI*}. The new configuration space defines a unique local fire behaviour, and is considered more suitable for investigating the fire regime transition. In other words, the present study elaborates the possible misuse of the conventional subjectively defined Byram convective number to

investigate practical fire behaviours. It is suggested that when wind speed is needed to calculate Byram convective number in real world, experimentalist should also take the vegetation properties into consideration that the reference height at which wind speed is measured should be based on the proposed mathematical expression.

Appendix

The governing equations of an inert vegetation version of the compressible solver ForestFireFoam (FFF, see [20]) is summarized as follows. Because solid volume fraction α_s is obtained from *CdLAI* and remain constant in the inert version of FFF, there is no need to evaluate gas volume fraction as $\alpha_g = 1 - \alpha_s$. The gas phase momentum equation is defined as,

$$\frac{\partial \alpha_g \bar{\rho} \widetilde{u_i}}{\partial \mathrm{t}} + \frac{\partial \alpha_g \bar{\rho} \widetilde{u_i} \widetilde{u_j}}{\partial \mathrm{x}_j} = -\frac{\partial \bar{p}}{\partial x_i} + \frac{\partial}{\partial x_j} \times \left(\alpha_g \bar{\rho} (\nu + \upsilon_t) \left(\frac{\partial \widetilde{u_i}}{\partial x_j} + \frac{\partial \widetilde{u_j}}{\partial x_i} - \frac{2}{3} \frac{\partial \widetilde{u_k}}{\partial x_k} \delta_{ij} \right) \right) + \alpha_g \bar{\rho} g_i - F_D \quad (1)$$

Where the drag force resulting from gas-solid interaction is given as,

$$F_D = \alpha_g \rho C_d \frac{\alpha_s \sigma_s}{2} |\tilde{u}| \widetilde{u_i} \quad (2)$$

An inert version of FFF does not take evaporation, pyrolysis and char oxidation rates into account leading to the following solid temperature T_s equation:

$$C_p^s \alpha_s \sigma_s \frac{dT_s}{dt} = Q_{rad}^s + Q_{conv}^s \quad (3)$$

Where $Q_{rad}^s = \alpha_s \sigma_s \times (J - T_s^4)$ and $Q_{conv}^s = h \alpha_s \sigma_s \times (T - T_s)$ are radiative and convective heat transfer from gas to solid, leading to an increase of solid temperature.

An enthalpy equation is written as,

$$\frac{\partial \alpha_g \bar{\rho} \widetilde{h}}{\partial \mathrm{t}} + \frac{\partial \alpha_g \bar{\rho} \widetilde{u_j} \widetilde{h}}{\partial \mathrm{x}_j} = -\frac{D\bar{p}}{Dt} + \frac{\partial}{\partial x_j} \times \left(\alpha_g \bar{\rho} \left(\alpha_D + \frac{\upsilon_t}{Pr_t} \right) \frac{\partial \widetilde{h}}{\partial x_j} \right) - Q_{conv}^s + Q_{rad} + Q_{comb} \quad (4)$$

Where the gas phase combustion and radiation energy Q_{comb} and Q_{rad} are calculated from a single step CO reaction model and a non-scattering, mean absorption-emission radiation model. In order to calculate Q_{rad} and Q_{rad}^s, the radiation intensity is obtained from solving a radiative heat transfer equation for a finite number of solid angles following:

$$\frac{d \alpha_g I_{rad}}{ds} = \alpha_g \gamma_0^g \left(\frac{\sigma T^4}{\pi} - I_{rad} \right) + \gamma_0^s \left(\frac{\sigma T_s^4}{\pi} - I_{rad} \right) \quad (5)$$

Where the first and second terms represent the contribution of radiation intensity from the gas and solid phase. The γ_0^g and γ_0^s represent the gas and solid absorption coefficient respectively. The total irradiance is then calculated as,

$$J = \int_0^{4\pi} I_{rad} d\Omega \quad (6)$$

The turbulent combustion is modelled using an improved EDC model that the gas phase chemical reaction rate is given as,

$$\overline{\dot{w}_F} = \frac{\bar{\rho}}{min(\frac{k_{sgs}}{C_{EDC}\varepsilon_{sgs}}, \frac{\Delta^2}{C_{DIFF}\alpha_{DIFF}})} min(\widetilde{Y_F}, \frac{\widetilde{Y_{O_2}}}{s}) \quad (7)$$

Where Y_F and Y_{O_2} are mass fraction of fuel and oxidizer respectively, and the *s* is the stoichiometric coefficient.

Declaration of conflicting interests

The authors declare that there is no conflict of interests.

Acknowledgements

This work is supported by Labex MEC (ANR-10-LABX-0092) and the A*MIDEX project (ANR-11-IDEX-0001-02), funded by the "Investissements d'Avenir".

This work was granted access to the HPC resources of Aix-Marseille University financed by the project Equip@Meso (ANR-10-EQPX-29-01) of the program "Investissements d'Avenir" supervised by the Agence Nationale pour la Recherche.

References

[1] Nelson, R.M., "Re-analysis of wind and slope effects on flame characteristics of Mediterranean shrub fires", *Int. J. Wildland Fire* 24:1001-1007 (2015).

[2] Pagni, P.J., Peterson, T.G., "Flame spread through porous fuels", *Proc. Comb. Inst.* 14:1099-1107 (1973).

[3] Nelson, R.M., Butler, B.W., Weise, D.R., "Entrainment regimes and flame characteristics of wildland fires", *Int. J. Wildland Fire* 21:127-140 (2012).

[4] Morandini, F., Silvani, X., 2010. Experimental investigation of the physical mechanisms governing the spread of wildfires. *Int. J. Wildland Fire* 19(5), pp.570-582.

[5] Catchpole, W.R., Catchpole, E.A., Butler, B.W., Rothermel, R.C., Morris, G.A. and Latham, D.J., "Rate of spread of free-burning fires in woody fuels in a wind tunnel", *Comb. Sci. and Tech.* 131:1-37 (1998).

[6] Cheney, N.P., Gould, J.S., Catchpole, W.R., "Prediction of fire spread in grasslands", *Int. J. Wildland Fire* 8:1-13 (1998).

[7] Morvan, D., Frangieh, N., "Wildland fires behaviour: wind effect versus Byram's convective number and consequences upon the regime of propagation", *Int. J. Wildland Fire* 27:636-641 (2018).

[8] Oke, T.R., Boundary Layer Climates, Routledge, 2002.

[9] Morvan, D., "Physical phenomena and length scales governing the behaviour of wildfires: a case for physical modelling", *Fire Tech*. 47:437-460 (2011).

[10] Morvan, D., Lamorlette, A., "Impact of solid fuel particle size upon the propagation of a surface fire through a homogeneous vegetation layer", *Fire Safety Sci.* 11:1326-1338 (2014).
[11] Morvan, D., Dupuy, J.L., "Modeling the propagation of a wildfire through a Mediterranean shrub using a multiphase formulation", *Comb. and Flame* 138:199-210 (2004).
[12] Morvan, D., Meradji, S., Accary, G., "Physical modelling of fire spread in grasslands", *Fire Safety J.* 44:50-61 (2009).
[13] Morvan, D., "Numerical study of the effect of fuel moisture content (FMC) upon the propagation of a surface fire on a flat terrain", *Fire Safety J* 58:121-131 (2013).
[14] Morvan, D., "Wind effects, unsteady behaviors, and regimes of propagation of surface fires in open field", *Comb. Sci. and Tech.*186:869-888 (2014).
[15] Morvan, D., "Numerical study of the behaviour of a surface fire propagating through a firebreak built in a Mediterranean shrub layer", *Fire Safety J* 71:34-48 (2015).
[16] Nicoud, F., Ducros, F., "Subgrid-scale stress modelling based on the square of the velocity gradient tensor", *Flow, Turb. and Comb.* 62:183-200 (1999).
[17] Magnussen, B.F., Hjertager, B.H., "On mathematical modeling of turbulent combustion with special emphasis on soot formation and combustion", *Proc. Comb. Inst.* 16:719-729 (1977).
[18] Verma S., Trouve A., "A study of the structure of a turbulent line fire subjected to cross-flow using large eddy simulations", *Proc 8th International Conference on Forest Fire Research*, Coimbra, Portugal, pp319-324.
[19] Ghisalberti, M., Nepf, H., The structure of the shear layer in flows over rigid and flexible canopies. *Env. Fluid Mech.* 6:277-301 (2006).
[20] El Houssami, M., Lamorlette, A., Morvan, D., Hadden, R.M., Simeoni, A., "Framework for submodel improvement in wildfire modeling", *Comb. and Flame* 190: 12-24 (2018).
[21] El Houssami, M., Thomas, J.C., Lamorlette, A., Morvan, D., Chaos, M., Hadden, R., Simeoni, A., "Experimental and numerical studies characterizing the burning dynamics of wildland fuels", *Comb. and Flame* 168:113-126 (2016).
[22] Syed, K.J., Stewart, C.D., Moss, J.B., "Modelling soot formation and thermal radiation in buoyant turbulent diffusion flames", *Proc. Comb. Inst.* 23:1533-1541 (1991).